

A mountain wind model for assisting fire management

Gary L. Achtemeier*

Center for Forest Disturbance Science
USDA Forest Service, Athens, GA

1. INTRODUCTION

Forestry organizations responsible for managing prescribed fire or controlling wildfire rely on weather forecasts of wind speed and wind direction for planning and allocation of resources. At the locations of fire sites in mountainous areas, winds are highly variable and may differ from winds at distant weather stations or from winds collected at safe sites just a few kilometers from fire lines. These uncertainties in winds can upset plans and place fire fighters in jeopardy. A number of methods to deduce spatial distributions of winds in mountainous terrain exist and it is not the purpose of this article to summarize them.

Among wind analysis methods in use among Forest Service users are mass conservative methods, and Wind Wizard (Forthofer, 2007; Forthofer, J. and B. Butler, 2007). Weise *et al.* (2007) used five methods for deducing wind speeds and directions (including Wind Wizard) for the Esperanza fire that burned 16137 hectares of chaparral and desert scrub vegetation in mountainous terrain in southern California on 26 October 2006. The methods varied in spatial resolution from none to the 100 m resolution of Wind Wizard. The resulting winds were input into the fire spread model, FARSITE (Finney, 1998) for simulating fire spread and compared with fire perimeters deduced from thermal imaging. The results confirmed that accurate wind data are critical if accurate predictions of fire spread are the operational goal.

In addition, there remains a need for a simple, fast, operationally adaptable model to simulate wind flow in mountainous terrain. Achtemeier (2003) derived a fire spread model based on a set of rules and simple equations cast as computer programs solved recursively (Wolfram, 2002). This model demonstrated skill in simulating complex coupled fire-atmosphere interactions and distributions of fire over landscapes. The proof-of-concept of a rule-driven mountain wind model (MWM) is the subject of this paper. The rule and its implementation are described in the next section. Results and discussion of MWM realism follow.

2. MATERIALS & METHODS

The MWM Rule M1 states that the impact of mountain barriers on wind fields can be described by a pressure function that is solved recursively. The

pressure function takes the form,

$$P = C_m \left(u \frac{\Delta z_s}{\Delta x} + v \frac{\Delta z_s}{\Delta y} \right) \quad (1)$$

where,

$$C_m = \frac{p_0 \Delta x}{c_0 R T_0} \quad (2)$$

where (u, v) are standard horizontal components of the vector wind, z_s is the elevation of the ground, R is the universal gas constant, Δx is the spacing of the model grid ($\Delta x = \Delta y$) and p_0 and T_0 are, respectively, reference pressure and temperature. The coefficient c_0 is a "stability time scale" that ensures convergence of the recursive solution.

Rule M1 was embedded within a modification of the wind model PB-Piedmont (Achtemeier, 2005). PB-Piedmont produces two-dimensional sigma layer-averaged winds draped over a landscape. Maximum resolution within PB-Piedmont determined by the resolution of the USGS national elevation data set is 30 m.

MWM was initialized with $\Delta x = 150 - 600$ m, $p_0 = 1212.5$ mb, $T_0 = 300^\circ\text{K}$. Simulations were done for a layer of depth 100 m draped over complex terrain. Mountains were replaced by the pressure function. However, winds were subjected to mass-weighted corrections. The solutions were not mass conservative.

Initial winds were set to zero. The wind field "spun up" in response to accelerations caused by the sum of the synoptic scale pressure field with the MWM pressure calculated from Equation (1). Objective interpolation of the NWS hourly surface pressures (reduced to sea level) provided the gridded synoptic scale pressure field (Achtemeier, 2005). As acceleration of the wind field is proportional to gradients of the pressure field, the solutions for the wind components are functions derivatives of the wind components – an inherently divergent problem. Thus to force convergence to a solution, c_0 was set to 50 s.

3. RESULTS & DISCUSSION

The MWM was run as a proof-of-concept experiment for four diverse mountainous terrains – an isolated mountain in Georgia, canyon lands in California, an Appalachian ridge in West Virginia, and terrain surrounding the location of the Esperanza fire in southern California. The results for each case are

* Corresponding author address: Gary L. Achtemeier, Forest Sciences Laboratory, 320 Green Street, Athens, GA 30602; e-mail: gachtemeier@fs.fed.us.

presented and discussed below.

a) Stone Mountain, Georgia

Stone Mountain, GA, is an isolated granite monolith, roughly parabolic in shape with length equal to 2,400 m and width equal to 960 m (Figure 1). The mountain is 500 m in elevation, roughly 235 m above surrounding flat land.

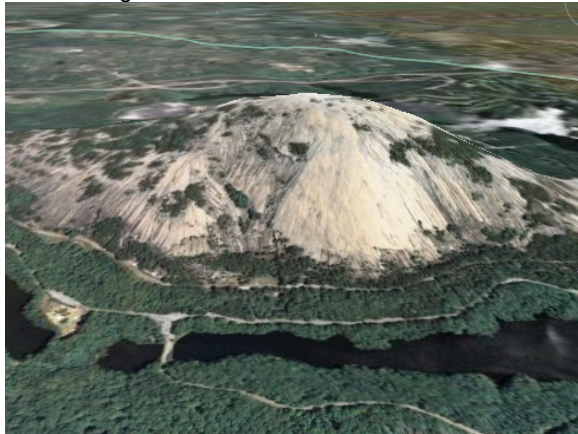


Figure 1. Stone Mountain, GA, looking north. The mountain is surrounded on three sides by lakes. (Image courtesy Google Earth)

An MWM solution for winds blowing from the south roughly normal to the major axis of Stone Mountain is shown in Figure 2. Grid spacing is 150 m. Winds of approximately 2.5 m sec^{-1} at [1] approaching the mountain slow to approximately 1 m sec^{-1} at [2] before accelerating to 5 m sec^{-1} at [3]. Then the winds decelerate rapidly to approximately 1 m sec^{-1} as the air flows down the steep north face of the mountain at [4].

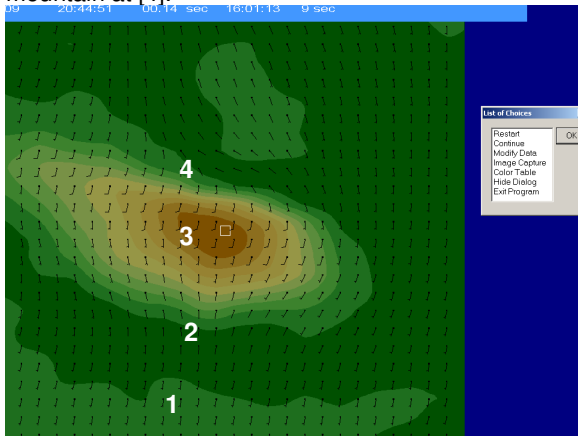


Figure 2. MWM solution for winds blowing from the south over Stone Mountain, GA. Long barb represents wind speed of 5 m sec^{-1} and short barb is 2.5 m sec^{-1} .

The solution bears qualitative resemblance to wind profiles observed at Askervein Hill, Scotland, (Taylor and Teunissen, 1983) which showed wind speed decrease during approach, followed by

increase to maximum winds near ridge top followed by sharp decrease along the downslope.

Figure 3 shows the MWM simulation for winds blowing along the major axis of Stone Mountain. The initially 2.5 m sec^{-1} flow diverges over the shoulder of the mountain beginning at [1] with no apparent deceleration. Maximum wind speeds of approximately 5 m sec^{-1} are found downwind of the peak at [2]. These winds decelerate and converge along the lee shoulder of Stone Mountain at [3].



Figure 3. Same as for Figure 2 except for winds blowing from the northwest along the axis of Stone Mountain.

b) Canyon Lands, California

The MWM Rule M1 was tested with complex terrain typical of that found in the Sierra Mountains of central California. Figure 4 shows flow over rugged terrain characterized by deep valleys. This site was chosen to show how Rule M1 forces air toward flowing up/down valleys. However, the flows are not confined in valleys as seen in the wind pattern near the center of the image.

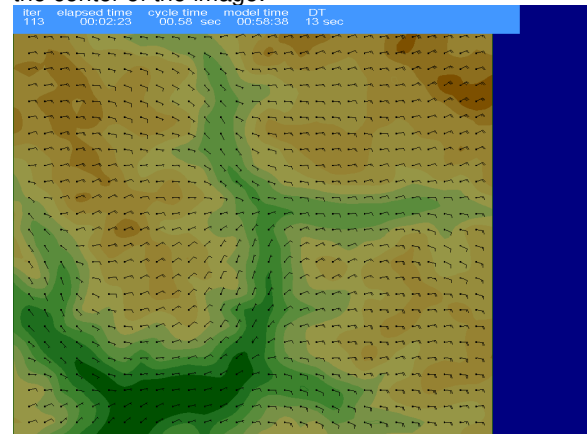


Figure 4. MWM solution for winds blowing over rugged terrain intercepted by steep valleys.

c) Ashwood Ridge, Virginia

The Appalachian Mountains over parts of eastern United States consist of long segmented

ridges. Figure 5 shows part of a 28 km unbroken ridge near Ashwood, VA. The ridge rises 400 m above the adjacent valley floors. An airport (KHSP) with a weather station is located on top of the ridge.



Figure 5. Part of a 400 m high ridge near Ashwood, VA. (Image courtesy Google Earth)

MWM was set up with a 600 m grid. Winds were simulated from 00 GMT 26 October 2006 through 00 GMT 30 October 2006. Results are summarized with the aid of the schematic in Figure 6. Winds blowing toward the ridge from an angle such as arrow [1] shifted to blow nearly parallel (but with a component toward the ridge) to the ridge and slowed as shown at arrow [2]. As the air drew closer to the ridge, the winds shifted with a large component normal to the ridge axis and increased in speed (arrow [3]). After crossing the ridge, winds shifted again to blow nearly parallel with the ridge but with a component directed toward lower elevation (arrow [4]). Winds speeds also decreased. At arrival at flat terrain, winds shifted to blow from the starting direction but with speeds generally less than starting speeds.

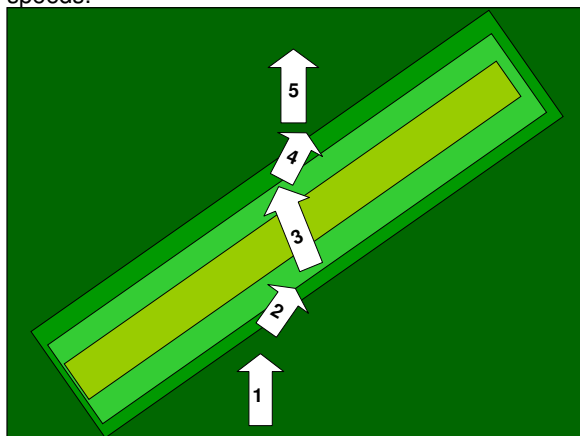


Figure 6. Schematic showing behavior of winds as they approach, cross, and depart a long unbroken ridge.

The sequence of winds turning to blow nearly parallel to a ridge, turning to blow normal to the ridge top, then turning to blow nearly parallel to the

ridge was found in varying degrees for all winds not blowing normal to or parallel to the axis of the ridge. Furthermore, the Rule M1 forcing at the ridge (arrow [3]) was so strong that as distant winds shifted from the east through the south, winds at the ridge top only shifted from ESE to SSE.

When the wind direction was parallel to the ridge, the winds at ridge top blew from that direction. However, when the winds blew from a direction not parallel to the ridge, the ridge top winds blew with a strong cross-ridge component. Figure 7 shows the behavior of wind direction during a wind shift at KHSP (blue line) on 28 October 2006. The wind shift began at 21 hours past 06 GMT 27 October 2006. The wind shifted from 140 degrees to 170 degrees after one hour then to 190 degrees after two hours. Wind directions held at 190 degrees for three hours before an abrupt shift to 260 degrees. The ridge is oriented at 215 degrees. The black line shows the Rule M1 solution. There is a shift of 100 degrees over three hours. Clearly one example does not make the case for Figure 6. Figure 7 does, however, give an example of wind shifts relative to ridge orientation that would be expected if Figure 6 describes actual wind behavior.

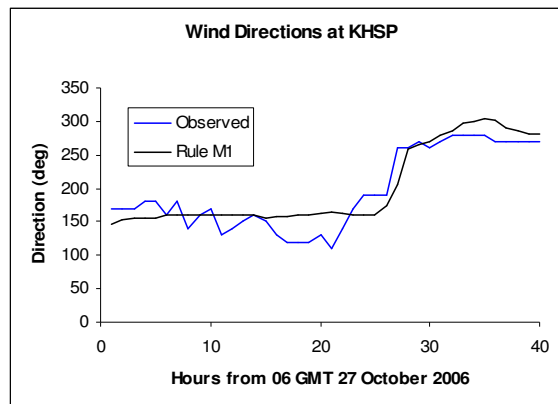


Figure 7. Wind directions at the top of the Ashwood ridge for a 40 hour period beginning 06 GMT 27 October 2006.

d) Esperanza Fire, California

In October 2006, the Esperanza wildfire consumed 16137 hectares of chaparral and desert scrub vegetation in mountainous terrain approximately 50 km east of Riverside, CA, (Weise *et al.*, 2007). Figure 8 shows terrain features that impacted winds during the fire. Terrain rose sharply from a flat valley of 500 m elevation to a rugged plateau that rose gradually from roughly 1000 m. A nearby mountain peaked at 1300 m. A range of higher mountains to the left of the image rose to 3200 m.



Figure 8. Site of the Esperanza fire looking south. Fire start location is given by the red ellipse. (Image courtesy Google Earth)

The Esperanza fire started at the base of the 1300 m mountain at midnight local standard time (17 GMT) 26 October 2006 and spread up the mountain while also being spread to the west by strong east winds blowing down the valley (green arrow). After having spread up the steep slopes at the edge of the valley, the fire was found in strong winds blowing from the northeast (blue arrow). These winds blew the fire up drainages with catastrophic effects. The combination of east winds on the valley floor and northeast winds over higher terrain was a major factor in the fire spread history of the Esperanza fire.

The MWM was set up with a 900 m grid that included the area of the fire, the valley and surrounding mountains out to 50 km from the fire. Surrounding NWS weather stations provided pressure observations needed for MWM. The objective was to determine the magnitude of impact of Rule M1 on winds transitioning from low to high terrain.

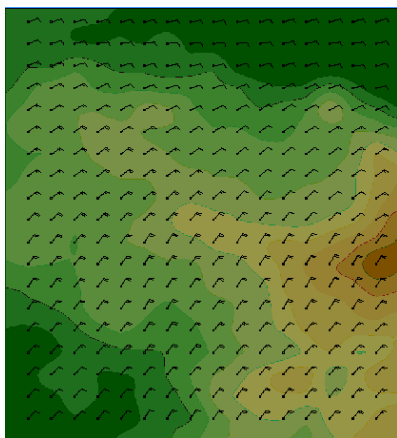


Figure 9. MWM simulated winds at 0800 LST 26 October 2006 for the domain of the Esperanza fire defined roughly by the blue arrow in Figure 8. North is at the top of the figure. The valley is the dark green area at the top of the figure and the 1300 m mountain appears as the brown shaded area at the right edge.

Figure 9 shows the wind field at 0800 LST for a subset of the model domain that includes areas most impacted by the Esperanza fire. The 1300 m mountain in Figure 8 is represented by the brown shaded area along the right edge of the map. Winds in the valley (dark green area at the top) are blowing from the east. Winds blowing from the valley toward higher elevation were simulated to blow from the northeast. Wind speeds increased with increasing elevation. Winds blowing in the valley at approximately 5 m sec^{-1} increased to greater than 10 m sec^{-1} over highest ground.

4. CONCLUSION

The Mountain Wind Model is a work in progress. The four cases described give illustrations of how Rule M1 impacts the wind field in mountainous terrain. The results are for 100 m layer averaged winds draped over complex terrain.

Because of the simplicity of Rule M1, the MWM in its current state, should produce inaccurate and unrealistic wind fields for the following conditions;

- 1) Complex three-dimensional wind fields that impact conditions at the ground,
- 2) Turbulent flows under high winds,
- 3) Flows at higher terrain where pressure observations currently used lose validity,
- 4) Light winds dominated by thermally-induced circulations,
- 5) Stable temperature strata, and
- 6) Probably more.

Furthermore, the solutions were carried out with stability time scale coefficient c_0 set globally. Plans are to repeat the simulations with the coefficient set locally as a function of terrain.

5. REFERENCES

Achtemeier, G.L., 2003: "Rabbit Rules" – An application of Stephen Wolfram's "new kind of science" to fire spread modeling. Extended abstract. Fifth Symp. Fire and Forest Meteor., Orlando, FL, Amer. Meteor. Soc.

Achtemeier, G.L., 2005: Planned Burn – Piedmont. A local operational numerical meteorological model for tracking smoke on the ground at night: Model development and sensitivity tests. *Int. J. Wildland Fire*, 14, 85-98.

Finney, M.A., 1998. FARSITE: Fire Area Simulator--Model Development and Evaluation. *USDA Forest Service Res. Paper RMRS-RP-4*, Rocky Mountain Research Station, Ft. Collins, Colorado.

Forthofer, J.M. 2007 (In prep.) Modeling wind in complex terrain for use in fire spread prediction. Fort Collins, CO: Colorado State University. (Expected completion 2007)

Forthofer, J. and B. Butler. 2007: Differences in Simulated Fire Spread Over Askervein Hill Using Two Advanced Wind Models and a Traditional Uniform Wind Field. In: Butler, B. W.; Cook, W., comps. 2007. The fire environment—innovations, management, and policy; conference proceedings. 26-30 March 2007; Destin, FL. Proceedings RMRS-P-46. Fort Collins, CO: U.S. Department of Agriculture, Forest Service, Rocky Mountain Research Station. 000 p. CD-ROM.

Taylor, P.A.; Teunissen, H.W. 1983. Askervein '82: Report on the September/October 1982 Experiment to study boundary layer flow over Askervein, South Uist. MSRB-83-8. Downsview, Ontario, CAN: Atmospheric Environment Service.

Weise, D. R., S. Chen, P. J. Riggan, F. M. Fujioka. 2007: Using high-resolution weather data to predict fire spread using the farsite simulator—a case study in California chaparral. Extended abstract. Seventh Symp. Fire and Forest Meteor., Bar Harbor, ME. Amer. Meteor. Soc. 10 pp.

Wolfram, S., 2002: A New Kind of Science. Wolfram Media, Inc., 1197 pp.